Numerical algorithm of the coupling ray theory in weakly anisotropic media

Petr Bulant & Luděk Klimeš
Department of Geophysics, Charles University, Ke Karlovu 3, 121 16 Praha 2, Czech Republic, Fax: +420-2-2191 1214,
E-mails: bulant@seis.karlov.mff.cuni.cz, klimes@seis.karlov.mff.cuni.cz

Summary

The paper is devoted to the numerical calculation of the frequency–dependent complex–valued vectorial amplitudes of S waves in weakly anisotropic media by the coupling ray theory. An efficient and accurate method of numerical integration of the coupling equation is proposed, and the accuracy of the method is estimated in order to control the integration step so that the relative error in the wavefield amplitudes due to the integration is kept below a given limit. Several quasi–isotropic approximations of the coupling ray theory are briefly discussed and a numerical example is presented.

Keywords

Coupling ray theory, anisotropy, travel times, amplitudes, Green function.

1 Introduction

There are two different high–frequency asymptotic ray theories, the *isotropic ray theory* assuming equal velocities of both S–wave polarizations and the *anisotropic ray theory* assuming both S–wave polarizations strictly decoupled.

In the isotropic ray theory, the S–wave polarization vectors do not rotate about the ray, whereas in the anisotropic ray theory, they coincide with the eigenvectors of the Christoffel matrix which may rotate rapidly about the ray.

In "weakly anisotropic" models, at moderate frequencies, the S–wave polarization tends to stay unrotated round the ray but is partly attracted by the rotation of the eigenvectors of the Christoffel matrix. The intensity of the attraction increases with frequency.

The isotropic and anisotropic ray theories are thus limiting cases and the gap between them has to be filled. A ray theory providing continuous transition between the isotropic and anisotropic ray theories was proposed by Coates & Chapman (1990) and is called the *coupling ray theory*. There are many possible modifications and approximations of the coupling ray theory. For example, the reference ray may be calculated in different ways (Bakker 2002), the Christoffel matrix may be approximated by its quasi–isotropic projections onto the plane perpendicular to the reference ray and onto the line tangent to the reference ray (Pšenčík 1998; Červený 2001), travel times corresponding to the anisotropic ray theory may be approximated in several ways, e.g., by linear quasi–isotropic perturbation with respect to the density–normalized elastic parameters (Pšenčík 1998; Červený 2001), etc. Several quasi–isotropic approximations of the coupling ray theory are briefly mentioned in Appendix A.

In: Seismic Waves in Complex 3-D Structures, Report 11 (Department of Geophysics, Charles University, Prague, 2001), pp. 263–277; to appear in Pure and Applied Geophysics, **159** (2002)

For comparison of isotropic, anisotropic and coupling ray theories with the exact solution in a simple model, refer to Bulant, Klimeš & Pšenčík (2000). The comparison also includes the quasi–isotropic approximation of the coupling ray theory by Pšenčík (1998), especially the effect of the quasi–isotropic approximation of travel times by linear perturbation with respect to the elastic parameters. The effect of the quasi–isotropic approximation of the Christoffel matrix is demonstrated on the numerical example in this paper.

This paper contains notes on the numerical calculation of the frequency–dependent complex–valued S–wave polarization vectors of the coupling ray theory. The method of numerical integration of the coupling equation, proposed by Červený (2001), is applied to the coupling equation derived by Coates & Chapman (1990), with emphasis on numerical implementation. The method of integration does not require the calculation of the angular velocity $\frac{\mathrm{d}\varphi}{\mathrm{d}\tau}$ of the rotation of the eigenvectors of the Christoffel matrix along the reference ray and does not require $\frac{\mathrm{d}\varphi}{\mathrm{d}\tau}$ to be smooth or finite along the reference ray. This is an important property, because the angular velocity of the rotation is undefined in the singular regions of the two equal eigenvalues of the Christoffel matrix.

The accuracy of the method of numerical integration of the coupling equation is estimated in Section 6 in order to control the integration step so that the relative error in the wavefield amplitudes due to the integration is kept below a given limit, which is of principal importance for numerical applications.

The calculation of P–wave travel–time perturbations from a reference isotropic model to an anisotropic model and the calculation of the S–wave coupling ray theory travel–time and amplitude corrections have been coded and added to the Fortran 77 package CRT (Klimeš 1998; Bucha & Klimeš 1999; Bucha, Bulant & Klimeš 2000). A simple numerical example of synthetic seismograms calculated by the coupling ray theory is presented.

2 Coupling ray theory for S waves

Assume a curve in phase space, hereinafter called the "reference ray", parametrized by reference travel time τ, with reference slowness vectors $p_i(\tau)$ known at all its points $x_j(\tau)$. The reference ray should be close to the ray of the wave under study. In particular, if shear wave coupling in weakly anisotropic media is investigated and the same reference ray is used for both S–wave polarizations, the reference ray should be close to the high–frequency approximations of the rays of both S waves (Bakker 2002).

Using the reference slowness vectors, we can calculate reference Christoffel matrices

$$\Gamma_{jk}(\tau) = p_i(\tau)\, a_{ijkl}\left(x_m(\tau)\right)\, p_l(\tau) \tag{1}$$

and their eigenvectors $g_{i1}(\tau)$, $g_{i2}(\tau)$, $g_{i3}(\tau)$ along the reference ray. Assume that eigenvectors $g_{i1}(\tau)$ and $g_{i2}(\tau)$ correspond to S waves and that they vary continuously along the reference ray. The continuity is not required in the regions where the corresponding two eigenvalues are equal. Let us denote $\tau_1(\tau)$ and $\tau_2(\tau)$ the travel times corresponding to polarizations $g_{i1}(\tau)$ and $g_{i2}(\tau)$, respectively. They may be approximated by quadratures along the unperturbed reference ray,

$$\frac{\mathrm{d}\tau_1}{\mathrm{d}\tau} = \left[\Gamma_{jk} g_{j1} g_{k1}\right]^{-\frac{1}{2}} \quad , \qquad \frac{\mathrm{d}\tau_2}{\mathrm{d}\tau} = \left[\Gamma_{jk} g_{j2} g_{k2}\right]^{-\frac{1}{2}} \quad . \tag{2}$$

For the derivation of (2) refer to Appendix B. The coupling ray theory solution u_i of the elastodynamic equations may then be expressed, for S waves, as a linear combination of the anisotropic ray theory solutions (Coates & Chapman 1990, eq. 15),

$$u_i = \sum_{M=1}^{2} g_{iM}\, A_M\, r_M \exp(\mathrm{i}\omega\tau_M) \quad , \tag{3}$$

where $A_M = A_M(\tau)$ are the complex–valued scalar amplitudes in the high–frequency approximation corresponding to polarizations g_{iM}. Because the amplitudes are calculated for the selected system of reference rays, using the relevant dynamic ray tracing along the reference ray (Červený 1972), they are identical, $A_M \equiv A = A(\tau)$. The coupling ray theory equation for complex–valued amplitude factors $r_M = r_M(\tau)$ reads (Coates & Chapman 1990, eq. 30)

$$\frac{\mathrm{d}}{\mathrm{d}\tau}\begin{pmatrix} r_1 \\ r_2 \end{pmatrix} = \frac{\mathrm{d}\varphi}{\mathrm{d}\tau}\begin{pmatrix} 0 & \exp\left(\mathrm{i}\omega[\tau_2(\tau)-\tau_1(\tau)]\right) \\ -\exp\left(\mathrm{i}\omega[\tau_1(\tau)-\tau_2(\tau)]\right) & 0 \end{pmatrix}\begin{pmatrix} r_1 \\ r_2 \end{pmatrix} \quad , \tag{4}$$

where

$$\frac{\mathrm{d}\varphi}{\mathrm{d}\tau} = g_{k2}\frac{\mathrm{d}g_{k1}}{\mathrm{d}\tau} = -g_{k1}\frac{\mathrm{d}g_{k2}}{\mathrm{d}\tau} \tag{5}$$

is the angular velocity of the eigenvector rotation. For several possible modifications and approximations of the above formulation of the coupling ray theory refer to Appendix A.

For high frequencies, $\exp\left(\mathrm{i}\omega[\tau_2(\tau)-\tau_1(\tau)]\right)$ in equation (4) may oscillate rapidly. These oscillations have minimal impact on the solution at high frequencies, because they cancel out after each period and the derivative of the solution is zero on average at high frequencies. However, these oscillations may either considerably reduce the accuracy, or increase the cost of the numerical integration.

In addition, travel times τ_M in equation (4) depend on the initial conditions. Equation (4) is thus much less suitable for defining the propagator matrix than equations with purely local coefficients.

The oscillation and global character of the coefficient matrix of equation (4) is caused by different travel times τ_M with respect to which the amplitude factors r_M are defined. Let us introduce new amplitude factors a_M, both related to the same "average" travel time $\overline{\tau}$ (Červený 2001),

$$r_1 \exp(\mathrm{i}\omega\tau_1) = a_1 \exp(\mathrm{i}\omega\overline{\tau}) \quad , \qquad r_2 \exp(\mathrm{i}\omega\tau_2) = a_2 \exp(\mathrm{i}\omega\overline{\tau}) \quad . \tag{6}$$

Inserting $r_M = a_M \exp\left(\mathrm{i}\omega[\overline{\tau}-\tau_M]\right)$ into equation (4), we obtain equation

$$\frac{\mathrm{d}}{\mathrm{d}\tau}\begin{pmatrix} a_1 \\ a_2 \end{pmatrix} = \left[\begin{pmatrix} 0 & 1 \\ -1 & 0 \end{pmatrix}\frac{\mathrm{d}\varphi}{\mathrm{d}\tau} - \mathrm{i}\omega\begin{pmatrix} \frac{\mathrm{d}(\overline{\tau}-\tau_1)}{\mathrm{d}\tau} & 0 \\ 0 & \frac{\mathrm{d}(\overline{\tau}-\tau_2)}{\mathrm{d}\tau} \end{pmatrix}\right]\begin{pmatrix} a_1 \\ a_2 \end{pmatrix} \quad . \tag{7}$$

It seems reasonable to simplify equation (7) by choosing

$$\overline{\tau}(\tau) = \tfrac{1}{2}[\tau_1(\tau)+\tau_2(\tau)] \quad . \tag{8}$$

Equation (7) then takes the form

$$\frac{\mathrm{d}}{\mathrm{d}\tau}\begin{pmatrix} a_1 \\ a_2 \end{pmatrix} = \left[\begin{pmatrix} 0 & 1 \\ -1 & 0 \end{pmatrix}\frac{\mathrm{d}\varphi}{\mathrm{d}\tau} - \begin{pmatrix} \mathrm{i} & 0 \\ 0 & -\mathrm{i} \end{pmatrix}\frac{\omega}{2}\frac{\mathrm{d}(\tau_2-\tau_1)}{\mathrm{d}\tau}\right]\begin{pmatrix} a_1 \\ a_2 \end{pmatrix} \quad . \tag{9}$$

3 Propagator matrix

Propagator matrix Π^g of equation (9), defined as

$$\Pi^g_{MN}(\tau,\tau_0) = \frac{\partial\, a_M(\tau)}{\partial\, a_N(\tau_0)} \quad , \tag{10}$$

is a complex–valued 2×2 matrix satisfying equation

$$\frac{\mathrm{d}}{\mathrm{d}\tau}\Pi^g = \left[\begin{pmatrix} 0 & 1 \\ -1 & 0 \end{pmatrix}\frac{\mathrm{d}\varphi}{\mathrm{d}\tau} - \begin{pmatrix} \mathrm{i} & 0 \\ 0 & -\mathrm{i} \end{pmatrix}\frac{\mathrm{d}\epsilon}{\mathrm{d}\tau}\right]\Pi^g \quad , \tag{11}$$

directly following from equation (9). Here

$$\epsilon(\tau) = \tfrac{1}{2}\omega\,[\tau_2(\tau) - \tau_1(\tau)] \quad . \tag{12}$$

Propagator matrix Π^g is symplectic and unitary, but we do not need to make use of these properties in this paper.

It is difficult to integrate equation (11) by the Runge–Kutta or another numerical method which requires derivative $\frac{\mathrm{d}\varphi}{\mathrm{d}\tau}$ along the reference ray to be calculated, because this derivative is undefined in the singular regions of the two equal eigenvalues of Christoffel matrix (1). For a more detailed discussion of the application of the Runge–Kutta methods to coupling equation (11) refer to Appendix D. The method of integration proposed in this paper does not require the calculation of derivative $\frac{\mathrm{d}\varphi}{\mathrm{d}\tau}$ and does not require the derivative to be smooth or finite along the reference ray.

Since Π^g is a propagator matrix satisfying the chain rule, it may be numerically calculated as the product of propagator matrices Π^g corresponding to reasonably small segments of the reference ray (Červený 2001). Frequency–dependent propagator matrices along individual small ray segments may be approximated with various degrees of accuracy and efficiency.

One of the possibilities how to approximate the local solutions, derived in more detail by the method of mean coefficients by Červený (2001), is suggested in this paper.

4 Analytic solution in a special case

Assume that $\frac{\mathrm{d}\varphi}{\mathrm{d}\tau} = \mathit{constant}\ \frac{\mathrm{d}\epsilon}{\mathrm{d}\tau}$, i.e. that $(\varphi-\varphi_0)/(\epsilon-\epsilon_0) = \mathit{constant}$. This assumption is used to derive a simple analytic solution of equation (11) within a small finite segment along the reference ray. The analytic solution will then be used to approximate the exact solution for variable ratio $(\varphi-\varphi_0)/(\epsilon-\epsilon_0)$ and the accuracy of the approximation will be studied in Section 6.

For $\frac{\mathrm{d}\varphi}{\mathrm{d}\tau} = \mathit{constant}\ \frac{\mathrm{d}\epsilon}{\mathrm{d}\tau}$, equation (11) takes the form

$$\tfrac{\mathrm{d}}{\mathrm{d}\tau}\Pi^g = \mathbf{A}\ \tfrac{\mathrm{d}\alpha}{\mathrm{d}\tau}\ \Pi^g \quad , \tag{13}$$

with constant matrix

$$\boxed{\mathbf{A} = \left[\begin{pmatrix} 0 & 1 \\ -1 & 0 \end{pmatrix}(\varphi-\varphi_0) - \begin{pmatrix} \mathrm{i} & 0 \\ 0 & -\mathrm{i} \end{pmatrix}(\epsilon-\epsilon_0)\right]\alpha^{-1}} \tag{14}$$

and parameter $\alpha = \alpha(\tau, \tau_0)$ defined as

$$\alpha = \sqrt{(\varphi - \varphi_0)^2 + (\epsilon - \epsilon_0)^2} \quad . \tag{15}$$

Here we have put $\varphi = \varphi(\tau)$, $\varphi_0 = \varphi(\tau_0)$, $\epsilon = \epsilon(\tau)$ and $\epsilon_0 = \epsilon(\tau_0)$. Since

$$\mathbf{A}^2 = -\mathbf{1} \quad , \tag{16}$$

the solution of equation (13) with unit initial conditions may be expressed in the form of

$$\Pi^g(\tau, \tau_0) = \exp(\mathbf{A}\alpha) = \mathbf{1}\cos(\alpha) + \mathbf{A}\sin(\alpha) \quad . \tag{17}$$

Note that equation (16), unlike (17), is valid exactly also for variable ratio $(\varphi - \varphi_0)/(\epsilon - \epsilon_0)$.

5 Approximation for short ray segments

We now use matrix (17) with (14) and (15) as the approximation for short ray segments, suggest how to calculate $\varphi - \varphi_0$ and $\epsilon - \epsilon_0$, and finally estimate the accuracy of the approximation.

Assume that vectors $g^0_{jM} = g_{jM}(\tau_0)$ are mapped onto vectors $g_{jM} = g_{jM}(\tau)$ in this way: (a) the vectors are rotated in plane $\mathrm{span}\{g^0_{j1}, g^0_{k2}\}$, (b) the vectors are rotated round the line of intersection of planes $\mathrm{span}\{g^0_{j1}, g^0_{k2}\}$ and $\mathrm{span}\{g_{j1}, g_{k2}\}$, (c) the vectors are rotated in plane $\mathrm{span}\{g_{j1}, g_{k2}\}$. The sum of the rotation angles in planes $\mathrm{span}\{g^0_{j1}, g^0_{k2}\}$ and $\mathrm{span}\{g_{j1}, g_{k2}\}$ is then given by

$$\Delta\varphi = \varphi - \varphi_0 = \arctan\left(\frac{g_{k1}g^0_{k2} - g_{k2}g^0_{k1}}{g_{k1}g^0_{k1} + g_{k2}g^0_{k2}}\right) \quad , \tag{18}$$

see (5). For the derivation of (18) refer to Appendix C.

Assume that travel times τ_M, $M = 1, 2$, can be obtained by trapezoidal quadratures of equations (2),

$$\Delta\tau_M = \tau_M(\tau) - \tau_M(\tau_0) \approx \tfrac{1}{2}\left[\ \tfrac{\mathrm{d}\tau_M}{\mathrm{d}\tau}(\tau) + \ \tfrac{\mathrm{d}\tau_M}{\mathrm{d}\tau}(\tau_0)\right]\Delta\tau \quad . \tag{19}$$

Equations (8) and (12) then yield

$$\Delta\overline{\tau} = \tfrac{1}{2}(\Delta\tau_2 + \Delta\tau_1) \tag{20}$$

and

$$\Delta\epsilon = \epsilon - \epsilon_0 = \tfrac{1}{2}\,\omega\,(\Delta\tau_2 - \Delta\tau_1) \quad . \tag{21}$$

6 Accuracy of the approximation

Equation (17) has been derived for constant ratio $(\varphi-\varphi_0)/(\epsilon-\epsilon_0)$ within the individual short ray segments, but is used as the numerical approximation of the exact solution for variable ratio $(\varphi-\varphi_0)/(\epsilon-\epsilon_0)$. We shall now estimate the accuracy of this numerical integration of coupling equation (11) in order to control the integration step so that the relative error in the wavefield amplitudes due to the integration is kept below a given limit.

The derivative of equation (17) along the reference ray reads

$$\tfrac{\mathrm{d}}{\mathrm{d}\tau}\Pi^g = \left[-\mathbf{1}\sin(\alpha)+\mathbf{A}\cos(\alpha)\right]\ \tfrac{\mathrm{d}\alpha}{\mathrm{d}\tau}+\ \tfrac{\mathrm{d}\mathbf{A}}{\mathrm{d}\tau}\sin(\alpha) \quad , \tag{22}$$

the matrix inverse to (17) is

$$[\Pi^g]^{-1} = \mathbf{1}\cos(\alpha)-\mathbf{A}\sin(\alpha) \tag{23}$$

and their product is

$$\tfrac{\mathrm{d}}{\mathrm{d}\tau}\Pi^g\ [\Pi^g]^{-1} = \mathbf{A}\ \tfrac{\mathrm{d}\alpha}{\mathrm{d}\tau}+\ \tfrac{\mathrm{d}\mathbf{A}}{\mathrm{d}\tau}\cos(\alpha)\sin(\alpha)-\ \tfrac{\mathrm{d}\mathbf{A}}{\mathrm{d}\tau}\mathbf{A}\left[\sin(\alpha)\right]^2 \quad . \tag{24}$$

The derivatives of α and $\mathbf{A}$ along the reference ray are

$$\tfrac{\mathrm{d}\alpha}{\mathrm{d}\tau} = \left[(\varphi-\varphi_0)\ \tfrac{\mathrm{d}\varphi}{\mathrm{d}\tau}+(\epsilon-\epsilon_0)\ \tfrac{\mathrm{d}\epsilon}{\mathrm{d}\tau}\right]\alpha^{-1} \tag{25}$$

and

$$\frac{\mathrm{d}\mathbf{A}}{\mathrm{d}\tau} = \left\{\begin{pmatrix}0&1\\-1&0\end{pmatrix}\left[\frac{\mathrm{d}\varphi}{\mathrm{d}\tau}-(\varphi-\varphi_0)\frac{\mathrm{d}\alpha}{\mathrm{d}\tau}\alpha^{-1}\right]-\begin{pmatrix}\mathrm{i}&0\\0&-\mathrm{i}\end{pmatrix}\left[\frac{\mathrm{d}\epsilon}{\mathrm{d}\tau}-(\epsilon-\epsilon_0)\frac{\mathrm{d}\alpha}{\mathrm{d}\tau}\alpha^{-1}\right]\right\}\alpha^{-1} \ . \tag{26}$$

Insertion of (25) and (15) into (26) yields

$$\frac{\mathrm{d}\mathbf{A}}{\mathrm{d}\tau} = \left[\begin{pmatrix}0&1\\-1&0\end{pmatrix}(\epsilon-\epsilon_0)+\begin{pmatrix}\mathrm{i}&0\\0&-\mathrm{i}\end{pmatrix}(\varphi-\varphi_0)\right]\left[(\epsilon-\epsilon_0)\frac{\mathrm{d}\varphi}{\mathrm{d}\tau}-(\varphi-\varphi_0)\frac{\mathrm{d}\epsilon}{\mathrm{d}\tau}\right]\alpha^{-3} \quad . \tag{27}$$

The product of (27) and (14) is

$$\tfrac{\mathrm{d}\mathbf{A}}{\mathrm{d}\tau}\mathbf{A} = \begin{pmatrix}0&\mathrm{i}\\\mathrm{i}&0\end{pmatrix}\left[(\epsilon-\epsilon_0)\ \tfrac{\mathrm{d}\varphi}{\mathrm{d}\tau}-(\varphi-\varphi_0)\ \tfrac{\mathrm{d}\epsilon}{\mathrm{d}\tau}\right]\alpha^{-2} \quad . \tag{28}$$

Now we subtract the matrix multiplying Π^g on the right–hand side of (11) from matrix $\mathbf{A}\ \tfrac{\mathrm{d}\alpha}{\mathrm{d}\tau}$ appearing on the right–hand side of (24). The coefficient with matrix $\begin{pmatrix}0&1\\-1&0\end{pmatrix}$ is

$$(\varphi-\varphi_0)\alpha^{-1}\ \tfrac{\mathrm{d}\alpha}{\mathrm{d}\tau}-\ \tfrac{\mathrm{d}\varphi}{\mathrm{d}\tau} = -(\epsilon-\epsilon_0)\left[(\epsilon-\epsilon_0)\ \tfrac{\mathrm{d}\varphi}{\mathrm{d}\tau}-(\varphi-\varphi_0)\ \tfrac{\mathrm{d}\epsilon}{\mathrm{d}\tau}\right]\alpha^{-2} \tag{29}$$

and the coefficient with matrix $\begin{pmatrix}\mathrm{i}&0\\0&-\mathrm{i}\end{pmatrix}$ is

$$-(\epsilon-\epsilon_0)\alpha^{-1}\ \tfrac{\mathrm{d}\alpha}{\mathrm{d}\tau}+\ \tfrac{\mathrm{d}\epsilon}{\mathrm{d}\tau} = -(\varphi-\varphi_0)\left[(\epsilon-\epsilon_0)\ \tfrac{\mathrm{d}\varphi}{\mathrm{d}\tau}-(\varphi-\varphi_0)\ \tfrac{\mathrm{d}\epsilon}{\mathrm{d}\tau}\right]\alpha^{-2} \quad . \tag{30}$$

Now we may insert equations (27)–(30) into (24) to calculate the deviation of the approximation from equation (11),

$$\frac{\mathrm{d}}{\mathrm{d}\tau}\Pi^g[\Pi^g]^{-1} - \left[\begin{pmatrix} 0 & 1 \\ -1 & 0 \end{pmatrix}\frac{\mathrm{d}\varphi}{\mathrm{d}\tau} - \begin{pmatrix} \mathrm{i} & 0 \\ 0 & -\mathrm{i} \end{pmatrix}\frac{\mathrm{d}\epsilon}{\mathrm{d}\tau}\right]$$
$$= \left\{\left[\begin{pmatrix} 0 & 1 \\ -1 & 0 \end{pmatrix}(\epsilon-\epsilon_0) + \begin{pmatrix} \mathrm{i} & 0 \\ 0 & -\mathrm{i} \end{pmatrix}(\varphi-\varphi_0)\right]\left[\cos(\alpha)\frac{\sin(\alpha)}{\alpha} - 1\right]\right.$$
$$\left. - \begin{pmatrix} 0 & \mathrm{i} \\ \mathrm{i} & 0 \end{pmatrix}[\sin(\alpha)]^2\right\}\left[(\epsilon-\epsilon_0)\frac{\mathrm{d}\varphi}{\mathrm{d}\tau} - (\varphi-\varphi_0)\frac{\mathrm{d}\epsilon}{\mathrm{d}\tau}\right]\alpha^{-2} \quad . \tag{31}$$

The relative error in Π^g per one step along a ray is then approximately matrix $\begin{pmatrix} 0 & \mathrm{i} \\ \mathrm{i} & 0 \end{pmatrix}$ times

$$\Delta\delta \approx -\int_{\tau_0}^{\tau}\left[(\epsilon-\epsilon_0)\frac{\mathrm{d}\varphi}{\mathrm{d}\tau} - (\varphi-\varphi_0)\frac{\mathrm{d}\epsilon}{\mathrm{d}\tau}\right]\mathrm{d}\tau = -\int_{\varphi_0}^{\varphi_0+\Delta\varphi}\left[(\epsilon-\epsilon_0) - (\varphi-\varphi_0)\,\frac{\mathrm{d}\epsilon}{\mathrm{d}\varphi}\right]\mathrm{d}\varphi \ . \tag{32}$$

Approximating $\epsilon-\epsilon_0$ by the second–order Taylor expansion with respect to $\varphi-\varphi_0$, we arrive at

$$(\epsilon-\epsilon_0) - (\varphi-\varphi_0)\,\tfrac{\mathrm{d}\epsilon}{\mathrm{d}\varphi} \approx -\tfrac{1}{2}\tfrac{\mathrm{d}^2\epsilon}{\mathrm{d}\varphi^2}(\varphi-\varphi_0)^2 \quad . \tag{33}$$

Within the second–order approximation (33), we can analytically integrate (32),

$$\Delta\delta \approx \frac{\mathrm{d}^2\epsilon}{\mathrm{d}\varphi^2}\frac{(\Delta\varphi)^3}{6} \approx \frac{(\Delta\varphi)^2}{6}\Delta\tfrac{\mathrm{d}\epsilon}{\mathrm{d}\varphi} \approx \frac{\Delta\varphi\Delta\tau}{6}\Delta\tfrac{\mathrm{d}\epsilon}{\mathrm{d}\tau} = \frac{\Delta\varphi\Delta\tau}{12}\omega\ \left(\Delta\,\tfrac{\mathrm{d}\tau_2}{\mathrm{d}\tau} - \Delta\,\tfrac{\mathrm{d}\tau_1}{\mathrm{d}\tau}\right) \ . \tag{34}$$

To keep the error in Π^g along the whole ray of length τ (measured in travel time) below the maximum specified limit, δ, we require

$$|\Delta\delta| \le \frac{\Delta\tau}{\tau}\ \delta \quad , \tag{35}$$

i.e.,

$$\boxed{|\Delta\varphi|\left|\Delta\frac{\mathrm{d}\tau_2}{\mathrm{d}\tau} - \Delta\frac{\mathrm{d}\tau_1}{\mathrm{d}\tau}\right| \le \frac{12}{\omega\tau}\ \delta \quad ,} \tag{36}$$

see (2). Note that, in addition to inequality (36), step $\Delta\varphi$ in the eigenvector rotation must also be sufficiently smaller than 45°,

$$|\Delta\varphi| \ll \frac{\pi}{4} \quad , \tag{37}$$

in order to reliably follow the selected eigenvector g_{kM} along the reference ray. Condition (37) need not be satisfied in the regions where the corresponding two eigenvalues are equal, i.e. where $\Delta\epsilon = 0$ within the required numerical accuracy. For example, there is no restriction on the selection of the eigenvectors of the Christoffel matrix in the isotropic parts of the model, while the proposed integration of the coupling equation is accurate. Inequality (36) can be satisfied in smooth models without problems, independently of the degree of anisotropy. The numerical integration with the integration step controlled by equations (36) and (37) has been coded and numerically tested.

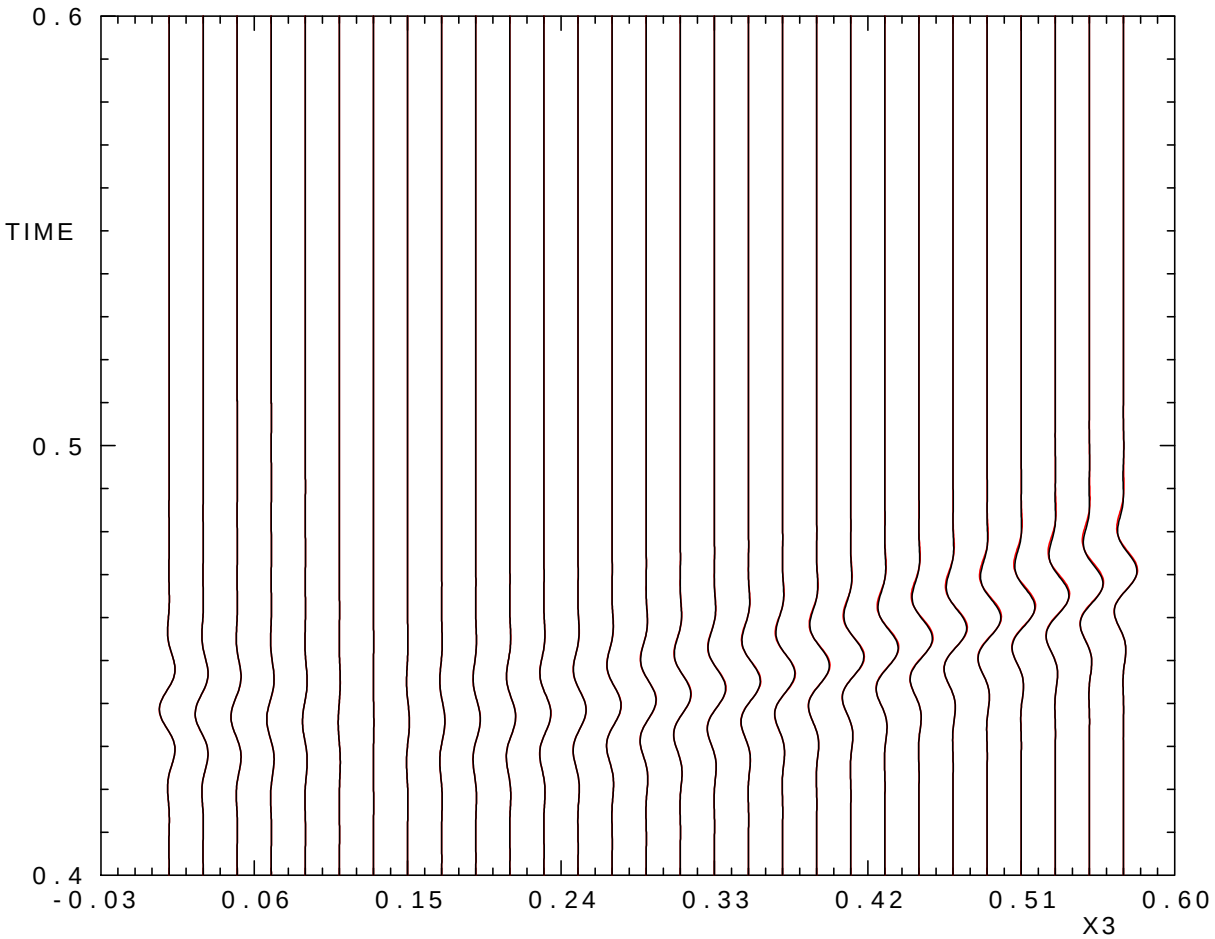

Figure 1. The first (radial) component of the coupling ray theory synthetic seismograms is shown in *black*. The *red* seismograms (somewhat obscured in this figure but better visible in Figure 2) correspond to the quasi–isotropic approximation of the Christoffel matrix, see also Figures 2 and 3.

7 Numerical example

The calculation of P–wave travel–time perturbations from a reference isotropic model to an anisotropic model and the calculation of the above described S–wave coupling ray theory travel–time and amplitude corrections along the isotropic reference rays have been coded in subroutine file `wan.for` and added to the Fortran 77 package CRT (Klimeš 1998; Bucha & Klimeš 1999; Bucha, Bulant & Klimeš 2000). The subroutines are called by program `green.for` if the model is anisotropic. In this case, program `green.for` generates frequency–dependent elementary Green functions (for S waves), further converted by program `greenss.for` into the response functions corresponding to a particular source radiation pattern. In the above cited versions of the code, the quasi–isotropic projection described in Subappendix A2 is applied at the source and receiver points.

A 1-D anisotropic model QI (model WA rotated by 45°) was provided by Pšenčík & Dellinger (2001) who performed the coupling ray theory calculations using the programs of package ANRAY and compared the results with the anisotropic reflectivity

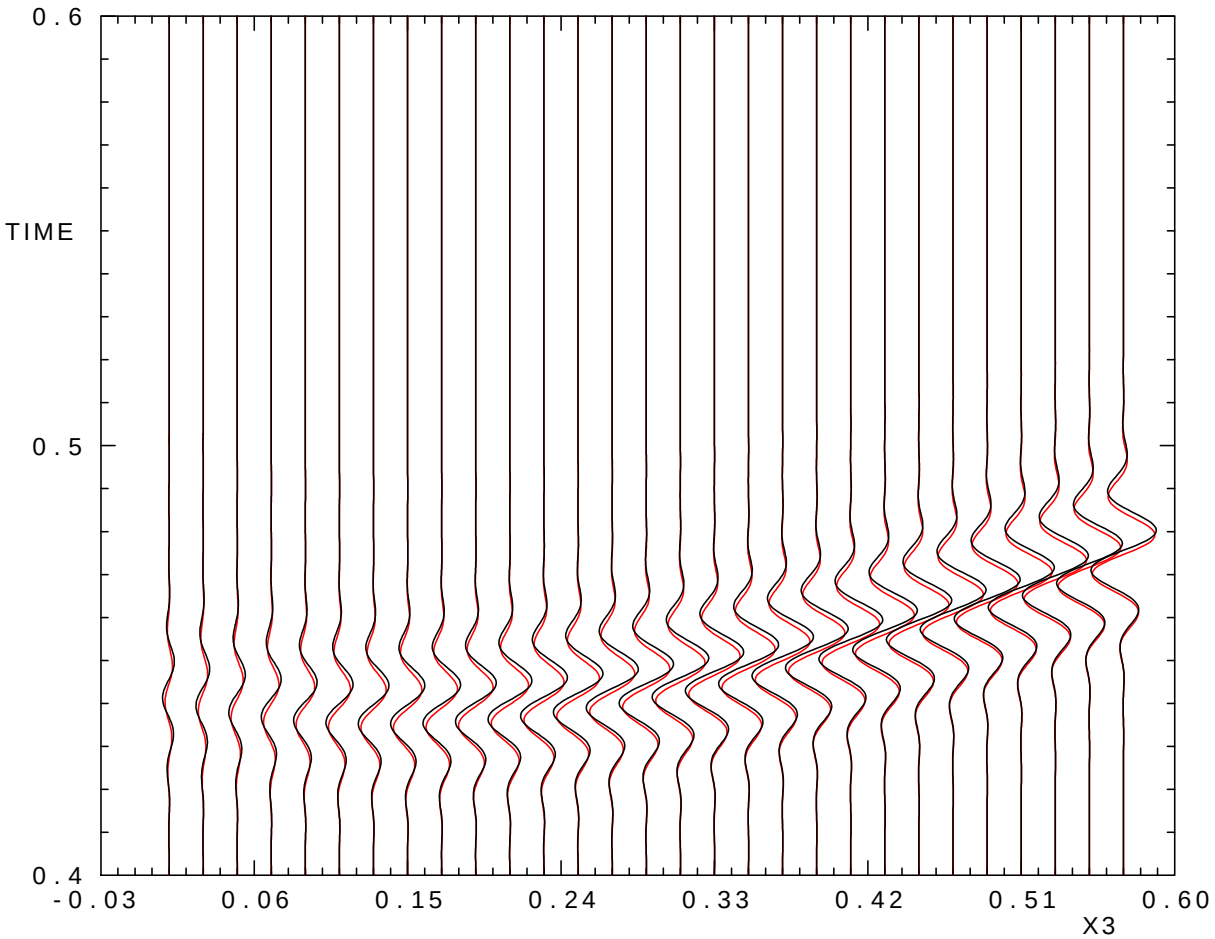

Figure 2. The second (transverse) component of the synthetic seismograms. Note that this component is zero in the one–dimensional reference isotropic model.

calculations. The normalized elastic parameters a_{ijkl} at the surface (zero depth) are

$$\begin{pmatrix} 14.48500 & 4.52500 & 4.75000 & 0.00000 & 0.00000 & -0.58000 \\ & 14.48500 & 4.75000 & 0.00000 & 0.00000 & -0.58000 \\ & & 15.71000 & 0.00000 & 0.00000 & -0.29000 \\ & & & 5.15500 & -0.17500 & 0.00000 \\ & & & & 5.15500 & 0.00000 \\ & & & & & 5.04500 \end{pmatrix} \tag{38}$$

and at the depth of 1 length unit they are

$$\begin{pmatrix} 22.08963 & 6.90063 & 7.24375 & 0.00000 & 0.00000 & -0.88450 \\ & 22.08953 & 7.24375 & 0.00000 & 0.00000 & -0.88450 \\ & & 23.95775 & 0.00000 & 0.00000 & -0.44225 \\ & & & 7.86138 & -0.26688 & 0.00000 \\ & & & & 7.86138 & 0.00000 \\ & & & & & 7.69363 \end{pmatrix} . \tag{39}$$

The reference isotropic model is given by

$$v_{\mathrm{P}}^2 = 15.00 \quad , \qquad v_{\mathrm{S}}^2 = 5.10 \tag{40}$$

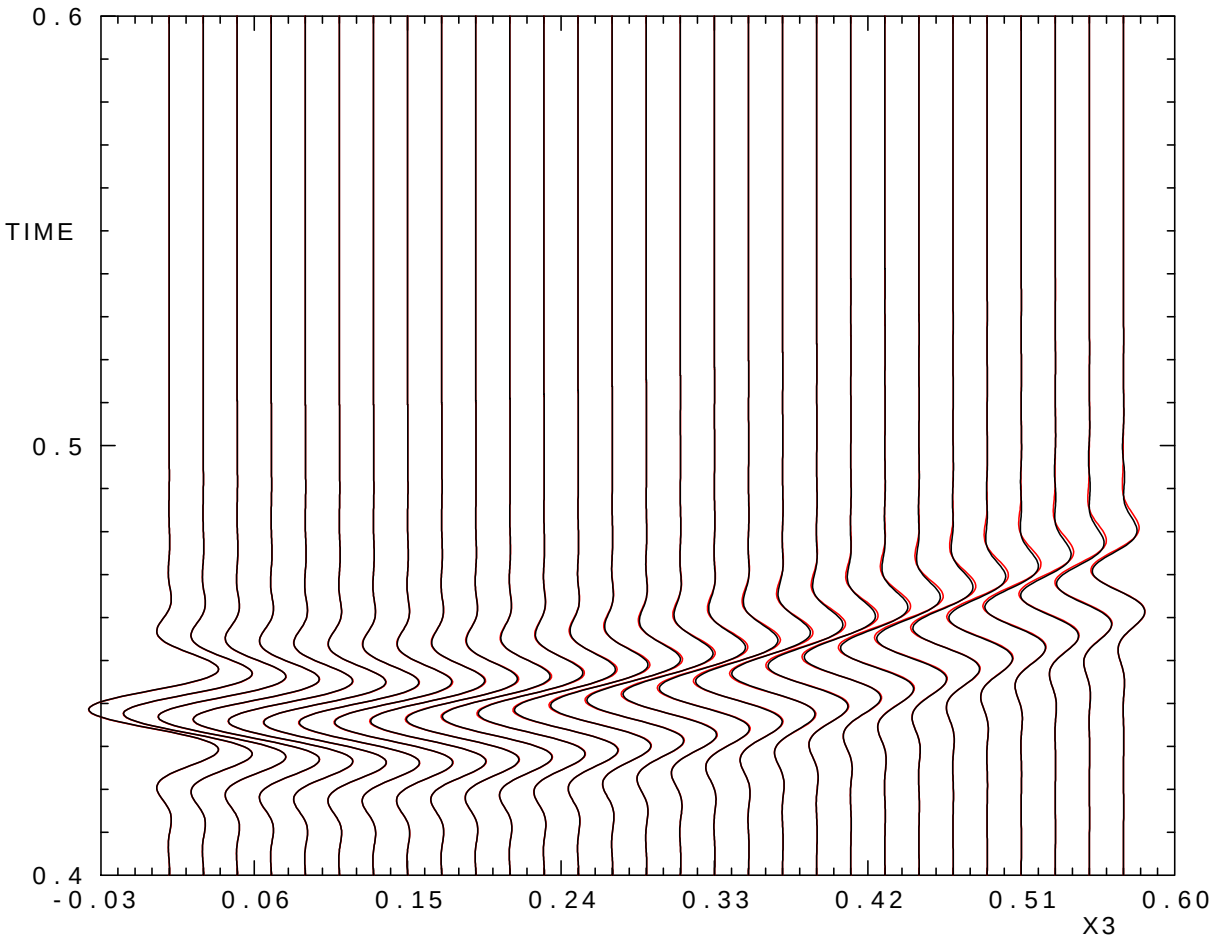

Figure 3. The third (vertical) component of the synthetic seismograms.

at the surface, and

$$v_{\mathrm{P}}^2 = 23.00 \quad , \qquad v_{\mathrm{S}}^2 = 7.79 \tag{41}$$

at the depth of 1 length unit. All the above values are interpolated linearly with depth. The homogeneous density is $\rho = 1$. The synthetic seismograms, corresponding to vertical force $\mathbf{F} = (0, 0, 100)^{\mathrm{T}}$ at position $(50, 50, 0)^{\mathrm{T}}$, are calculated at 29 receivers $(51, 50, 0.010)^{\mathrm{T}}$, $(51, 50, 0.030)^{\mathrm{T}}$, $(51, 50, 0.050)^{\mathrm{T}}$, ..., $(51, 50, 0.570)^{\mathrm{T}}$ located in a vertical well. The source time function is the Gabor signal $\cos(2\pi f t)\exp[-(2\pi f t/4)^2]$ with reference frequency $f = 50\,\mathrm{Hz}$, band–pass filtered by the cosine filter given by frequencies $0\,\mathrm{Hz}$, $5\,\mathrm{Hz}$, $60\,\mathrm{Hz}$ and $100\,\mathrm{Hz}$.

The resulting coupling ray theory seismograms, modified by the quasi–isotropic projection of Subappendix A2, are plotted in Figures 1, 2 and 3 in black. The maximum polarization error of the quasi–isotropic projection is 0.061 radians in this example. For comparison, the seismograms calculated according to the quasi–isotropic approximation of Subappendix A3 (corresponding to the seismograms calculated by package ANRAY) are plotted in red. The effect of the quasi–isotropic approximation of Subappendix A4 is negligible in this example. On the other hand, the effect of the quasi–isotropic approximation of Subappendix A4 has been demonstrated by Bulant, Klimeš & Pšenčík (2000) in a simple model in which the quasi–isotropic approximation of Subappendix A3 does not affect the results.

The model is named QI and the data for packages CRT and ANRAY may be found on compact disks Klimeš (1998), Bucha & Klimeš (1999) and Bucha, Bulant & Klimeš (2000), together with the Fortran 77 source code of the packages. For comparison with the isotropic and anisotropic ray theory seismograms and for a more detailed discussion and description of this model refer to Pšenčík & Dellinger (2001).

8 Conclusions

The proposed numerical algorithm for the coupling ray theory is very efficient and accurate, with controlled accuracy. It requires negligible computational time because the coupling equation is solved only along the previously calculated two–point rays. In weakly anisotropic media, the coupling ray theory should be much more accurate than the isotropic and anisotropic ray theories, although its actual accuracy and limits of applicability are still unknown.

Appendix A: Quasi–isotropic approximations of the coupling ray theory

A1 Selection of the reference ray

The isotropic ray theory is always the limiting case of the coupling ray theory for decreasing anisotropy at fixed frequency. On the other hand, the high–frequency limit of the coupling ray theory at fixed anisotropy depends on the choice of the reference ray, and even on the choice of the *system* of reference rays, because the amplitudes are determined by the paraxial reference rays.

If we choose the *anisotropic ray theory reference ray* and select the initial polarization corresponding to the reference ray, the coupling ray theory will correctly limit to the anisotropic ray theory for high–frequencies. For other choices of reference rays, the high–frequency limit of the coupling ray theory at fixed anisotropy is incorrect, although the differences may be negligible at the finite frequencies under consideration.

In the *anisotropic common–ray approximation*, the common reference ray is traced using the averaged Hamiltonian of both S–wave polarizations (Bakker 2002).

In the less accurate *isotropic common–ray approximation*, the reference ray is traced in the reference isotropic model. Moreover, the reference isotropic model may be selected in different ways, yielding quasi–isotropic approximations of various accuracy.

A2 Quasi–isotropic projection of the polarization vectors

The coupling ray theory solution (3) may be approximated by its projection

$$\tilde{u}_i = h_{iM} h_{mM} u_m \tag{A1}$$

onto the orthonormal reference polarization vectors h_{k1}, h_{k2}. This approximation may simplify the modification of existing isotropic ray tracing codes for the coupling ray theory. The error of this approximation is obvious and can be calculated simply.

A3 Quasi–isotropic approximation of the Christoffel matrix

Denote the polarization vectors of the isotropic ray theory, or the reference polarization vectors in general, by h_{k1}, h_{k2} and h_{k3}. If the Christoffel matrix is approximated by its projections onto plane span$\{h_{j1}, h_{k2}\}$ and onto vector h_{l3},

$$\begin{aligned}\tilde{\Gamma}_{jk} &= h_{jM}h_{mM}\Gamma_{mn}h_{nN}h_{kN} + h_{j3}h_{m3}\Gamma_{mn}h_{n3}h_{k3} \\ &= \Gamma_{jk} - (h_{jM}h_{k3} + h_{j3}h_{kM})h_{mM}\Gamma_{mn}h_{n3} \quad , \end{aligned} \tag{A2}$$

eigenvectors g_{k1} and g_{k2} become situated in plane span$\{h_{j1}, h_{k2}\}$ as in the zero-order quasi–isotropic approximation of Pšenčík (1998) and Červený (2001). This approximation includes the approximation of Subappendix A2.

A4 Quasi–isotropic perturbation of travel times

The linearized perturbation of equations (2) with respect to the density–normalized elastic parameters yields approximation

$$\frac{\mathrm{d}\tau_1}{\mathrm{d}\tau} \approx (\Gamma^0_{jk}g_{j1}g_{k1})^{-\frac{1}{2}} - \frac{1}{2}(\Gamma_{jk} - \Gamma^0_{jk})g_{j1}g_{k1}(\Gamma^0_{jk}g_{j1}g_{k1})^{-\frac{3}{2}} \quad . \tag{A3}$$

Assuming that

$$\Gamma^0_{jk}g_{j1}g_{k1} = 1 \quad , \tag{A4}$$

see Subappendix A3, equation (A3) reads

$$\frac{\mathrm{d}\tau_1}{\mathrm{d}\tau} \approx \frac{3}{2} - \frac{1}{2}\Gamma_{jk}g_{j1}g_{k1} \quad , \tag{A5}$$

as in the quasi–isotropic approximation of Pšenčík (1998) and Červený (2001). Analogously for $\frac{\mathrm{d}\tau_2}{\mathrm{d}\tau}$. The quasi–isotropic perturbation of travel times leads to an erroneous time shift in synthetic seismograms but has a negligible impact on the amplitudes.

Appendix B: Derivation of equations (2)

We present the derivation for $\frac{\mathrm{d}\tau_1}{\mathrm{d}\tau}$, equations for $\frac{\mathrm{d}\tau_2}{\mathrm{d}\tau}$ are analogous. The derivation is based on the assumption that equation

$$\tau_1 = \tau_1(\tau) \tag{B1}$$

can be applied approximately also in the vicinity of the reference ray. Equation (B1) means that the gradient of τ_1 is parallel to the gradient of τ in the vicinity of the reference ray. The Christoffel matrix corresponding to travel time τ_1 is then

$$\frac{\partial\tau_1}{\partial x_i}\, a_{ijkl}\, \frac{\partial\tau_1}{\partial x_l} = \left[\frac{\mathrm{d}\tau_1}{\mathrm{d}\tau}\right]^2 \Gamma_{jk}(\tau) \quad , \tag{B2}$$

and has the same eigenvectors as the reference Christoffel matrix $\Gamma_{jk}(\tau)$ defined by equation (1). The eigenvalue of Christoffel matrix (B2) corresponding to the eigenvector $g_{i1}(\tau)$ has to be unity,

$$\left[\frac{\mathrm{d}\tau_1}{\mathrm{d}\tau}\right]^2 \Gamma_{jk}(\tau)g_{j1}(\tau)g_{k1}(\tau) = 1 \quad , \tag{B3}$$

which yields equations (2).

Appendix C: Derivation of equation (18)

Denote by e_{j1} the unit vector along the line of intersection of planes span$\{g^0_{j1}, g^0_{k2}\}$ and span$\{g_{j1}, g_{k2}\}$. Denote by e^0_{j2} and e_{j2} unit vectors perpendicular to e_{j1} in planes span$\{g^0_{j1}, g^0_{k2}\}$ and span$\{g_{j1}, g_{k2}\}$, respectively.

We assume that

(a) vectors g^0_{j1}, g^0_{j2} are rotated about vector g^0_{j3}, perpendicular to plane span$\{g^0_{j1}, g^0_{k2}\}$, through angle φ_1 to reach vectors e_{j1}, e^0_{j2},

$$(e_{j1}, e^0_{j2}, g^0_{j3}) = (g^0_{j1}, g^0_{j2}, g^0_{j3}) \begin{pmatrix} \cos\varphi_1 & -\sin\varphi_1 & 0 \\ \sin\varphi_1 & \cos\varphi_1 & 0 \\ 0 & 0 & 1 \end{pmatrix} \quad , \tag{C1}$$

(b) vectors e^0_{j2}, g^0_{j3} are rotated about vector e_{j1} through angle α to reach vectors e_{j2}, g_{j3},

$$(e_{j1}, e_{j2}, g_{j3}) = (e_{j1}, e^0_{j2}, g^0_{j3}) \begin{pmatrix} 1 & 0 & 0 \\ 0 & \cos\alpha & -\sin\alpha \\ 0 & \sin\alpha & \cos\alpha \end{pmatrix} \quad , \tag{C2}$$

(c) vectors e_{j1}, e_{j2} are rotated about vector g_{j3}, perpendicular to plane span$\{g_{j1}, g_{k2}\}$, through angle φ_2 to reach vectors g_{j1}, g_{j2},

$$(g_{j1}, g_{j2}, g_{j3}) = (e_{j1}, e_{j2}, g_{j3}) \begin{pmatrix} \cos\varphi_2 & -\sin\varphi_2 & 0 \\ \sin\varphi_2 & \cos\varphi_2 & 0 \\ 0 & 0 & 1 \end{pmatrix} \quad . \tag{C3}$$

Then

$$\begin{pmatrix} g_{j1}g^0_{j1} & g_{j2}g^0_{j1} \\ g_{j1}g^0_{j2} & g_{j2}g^0_{j2} \end{pmatrix} = \begin{pmatrix} \cos\varphi_1 & -\sin\varphi_1 \\ \sin\varphi_1 & \cos\varphi_1 \end{pmatrix} \begin{pmatrix} 1 & 0 \\ 0 & \cos\alpha \end{pmatrix} \begin{pmatrix} \cos\varphi_2 & -\sin\varphi_2 \\ \sin\varphi_2 & \cos\varphi_2 \end{pmatrix}$$
$$= \begin{pmatrix} \cos\varphi_1\cos\varphi_2 - \sin\varphi_1\cos\alpha\sin\varphi_2 & -\cos\varphi_1\sin\varphi_2 - \sin\varphi_1\cos\alpha\cos\varphi_2 \\ \sin\varphi_1\cos\varphi_2 + \cos\varphi_1\cos\alpha\sin\varphi_2 & -\sin\varphi_1\sin\varphi_2 + \cos\varphi_1\cos\alpha\cos\varphi_2 \end{pmatrix} . \tag{C4}$$

We see that

$$g_{j1}g^0_{j2} - g_{j2}g^0_{j1} = (1+\cos\alpha)\sin(\varphi_1+\varphi_2) \tag{C5}$$

and

$$g_{j1}g^0_{j1} + g_{j2}g^0_{j2} = (1+\cos\alpha)\cos(\varphi_1+\varphi_2) \quad , \tag{C6}$$

which yields equation (18) for the sum

$$\Delta\varphi = \varphi_1 + \varphi_2 \tag{C7}$$

of rotation angles.

Appendix D: Comparison with the Runge–Kutta methods

Coupling equation (11) can be solved by a Runge–Kutta method if the first derivative $\frac{\mathrm{d}\varphi}{\mathrm{d}\tau}$ of rotation angle $\varphi(\tau)$ is smooth and finite, whereas the method proposed in this paper requires nothing but condition (37) and only outside the singular regions.

The numerical integration of coupling equation (11) by a Runge–Kutta method requires the derivative (5) of rotation angle $\varphi(\tau)$ to be calculated. The calculation of this derivative is much more involved than the calculation of angular increment (18), and fails in the singular regions where the Christoffel matrix has two equal eigenvalues.

To efficiently control the accuracy, the Runge–Kutta methods have to be applied with a variable step along the reference ray, similarly as the method proposed in this paper. Unfortunately, the correct length of the integration step of the Runge–Kutta method cannot be determined reliably in advance. The variable step is also the reason why the predictor–corrector methods, designed primarily for a regular step, are not considered.

To keep the error of the fourth–order Runge–Kutta method with the integration step composed of two equal half–steps $\Delta\tau$ (Ralston 1965, eq. 5.6-48) below the maximum specified limit δ, the very roughly derived condition

$$\frac{\alpha^5}{\Delta\tau} \leq \frac{1}{\tau}\frac{45}{73}\,\delta \tag{D1}$$

should be satisfied. Here α is defined by equations (15), (18) and (12). Condition (D1) is always more restrictive than condition (37). At high frequencies, condition (36) implies proportionality $\Delta\tau \sim \omega^{-\frac{1}{2}}$, whereas condition (D1) implies proportionality $\Delta\tau \sim \omega^{-\frac{5}{4}}$. That is why the fourth–order Runge–Kutta method requires shorter integration steps than the method proposed in this paper at high frequencies, at which the two S–wave polarizations are split.

Runge–Kutta methods of lower orders are much less efficient than the fourth–order Runge–Kutta method for the numerical solution of the coupling equation at all frequencies.

Acknowledgements

The authors thank Ivan Pšenčík for his essential cooperation during the preparation of the paper and both anonymous reviewers for their suggestions enabling to improve the manuscript considerably.

This research has been supported by the Grant Agency of the Czech Republic under Contract 205/01/0927, by the Ministry of Education of the Czech Republic within Research Project J13/98 113200004, and by the members of the consortium "Seismic Waves in Complex 3-D Structures" (see "http://seis.karlov.mff.cuni.cz/consort/main.htm").

References

Bakker, P.M. (2002): Coupled anisotropic shear wave raytracing in situations where associated slowness sheets are almost tangent. Pure appl. Geophys., **159**, in press.

Bucha, V., Bulant, P. & Klimeš, L. (eds.) (2000): SW3D–CD–4. In: Seismic Waves in Complex 3-D Structures, Report 10, p. 227, Dep. Geophys. Charles Univ., Prague, online at "http://seis.karlov.mff.cuni.cz/software/sw3dcd4/index.htm".

Bucha, V. & Klimeš, L. (eds.) (1999): SW3D–CD–3. In: Seismic Waves in Complex 3-D Structures, Report 8, p. 193, Dep. Geophys. Charles Univ., Prague, online at "http://seis.karlov.mff.cuni.cz/software/sw3dcd3/index.htm".

Bulant, P., Klimeš, L. & Pšenčík, I. (2000): Comparison of ray methods with the exact solution in the 1-D anisotropic "twisted crystal" model. Expanded Abstracts of 70th Annual Meeting (Calgary), Soc. Explor. Geophysicists, Tulsa, pp. 2289–2292.

Červený, V. (1972): Seismic rays and ray intensities in inhomogeneous anisotropic media. Geophys. J. R. astr. Soc., **29**, 1–13.

Červený, V. (2001): Seismic Ray Theory. Cambridge Univ. Press, Cambridge.

Coates, R.T. & Chapman, C.H. (1990): Quasi–shear wave coupling in weakly anisotropic 3-D media. Geophys. J. int., **103**, 301–320.

Klimeš, L. (ed.) (1998): SW3D–CD–2. In: Seismic Waves in Complex 3-D Structures, Report 7, p. 405, Dep. Geophys. Charles Univ., Prague, online at "http://seis.karlov.mff.cuni.cz/software/sw3dcd2/index.htm".

Pšenčík, I. (1998): Green's functions for inhomogeneous weakly anisotropic media. Geophys. J. int., **135**, 279–288.

Pšenčík, I. & Dellinger. J. (2001): Quasi–shear waves in inhomogeneous weakly anisotropic media by the quasi–isotropic approach: A model study. Geophysics, **66**, 308–319.

Ralston, A. (1965): A First Course in Numerical Analysis. McGraw-Hill, New York.